

DFT Versus the “Real World” (or, Waiting for Godft)

Peter J. Feibelman

Published online: 10 April 2010
© Sandia National Labs 2010

Abstract “Real-world” problems, from the properties of synthetic, nano-structured materials to the nature of bio-materials’ interactions, tax the capabilities of modern, approximate Density Functional Theory (DFT) methods. And, progress is often illusory; that is, an “improved” functional can describe systems of interest *less* faithfully than an older, “cruder” one. Examples discussed concern water at hydrophilic surfaces, and the morphology of nano-clusters grown on a graphene-on-precious-metal template. The results suggest that in the absence of considerable prior insight, where energy differences are small, applying DFT to decipher the meaning of well-characterized experimental data is apt to be more successful than to predict molecular-level structure.

Keywords Density functional theory (DFT) · Water · Ice · Hydrophilic · Wetting · Ruthenium · Dissociation · Palladium · Strain · Commensurate · Platinum · AgI · Cloud · Seeding · Graphene · Iridium · Cluster · Array · Template · Growth · Scanning tunneling microscopy (STM) · Low energy electron diffraction (LEED)

This manuscript has been authored by Sandia Corporation under Contract No. DE-AC04-94AL85000 with the U.S. Department of Energy. The United States Government retains and the publisher, by accepting the article for publication, acknowledges that the United States Government retains a non-exclusive, paid-up, irrevocable, world-wide license to publish or reproduce the published form of this manuscript, or allow others to do so, for United States Government purposes.

P. J. Feibelman (✉)
Sandia National Laboratories, Albuquerque,
NM 87185-1415, USA
e-mail: pjfeibe@sandia.gov

1 Introduction

Before embarking on a scientific endeavor, it makes sense to ask if the project is “timely.” To the novice, there is no obvious difference between timeliness and importance. To a researcher whose biography includes spending far too much effort *failing* to resolve an important problem, the distinction is painfully clear: Even an important problem is not timely until appropriate technical infrastructure is in place.

Prior to the invention of the Scanning Tunneling Microscope (STM) [1], for example, deciphering even a modestly complicated surface structure was a serious challenge. The most highly developed technique was to vary atomic positions to achieve a best fit to Low Energy Electron Diffraction, intensity versus voltage data. The scattering theory used to do this, however, embodied systematic errors whose magnitude were not easily quantified, and besides, given the computer power of the day, the analysis was very time-consuming for all but the most “ideal” problems (i.e., those with the smallest surface unit cells).¹

Under the circumstances, one could hardly imagine applying surface structure information to the design of an improved catalyst. One could barely agree on the spacing between the first two layers of a metal crystal surface! Promised applications of surface science therefore stayed “on the back burner.”

Once the STM was available, the years of structure analysis were foreshortened, and surface science matured. With the STM in place, defective surfaces, and periodic ones with large unit cells, like the Si(111)— 7×7 surface, which had stood as a virtual Everest to conquer, could be

¹ For a historical perspective, See Ref. [2].

imaged and understood.² Surface problems of interest to catalytic chemists or device physicists became timely, which had not been before.

For the surface theorist, timeliness is no less an issue. Enormous advances in computational power, and the Nobel-winning invention of Density Functional Theory (DFT) [4, 5], have made insight achievable into the structure and dynamics of molecules, surfaces and bulk condensed-matter, even in the face of hard-to-quantify, systematic error in today's functionals.

It is not surprising that DFT's successes mainly involve systems governed by chemical (i.e., strong) forces, and correspondingly large energy differences. For them, the inherent systematic error in the approximate functionals is small enough (apparently). Is current approximate DFT applicable to "real-world" problems, e.g., of living things, running at ambient temperature and pressure? If not, applying DFT to a real-world problem, even a very important one, is a *quixotic* endeavor, not a timely one. The risk is spending a great deal of effort, fruitlessly applying an insufficiently advanced technique.

2 Half-Dissociated Water on Ru(0001)

With such thoughts in mind, about eight years ago, I set out to learn whether DFT calculations could help to interpret what was then the only published, quantitative experimental structure of a water monolayer on a single-crystal surface. Held and Menzel had gathered and analyzed Low Energy Electron Diffraction (LEED) intensity vs. voltage data for $\sqrt{3} \times \sqrt{3} - R30^\circ$ D₂O/Ru(0001), and had come to the surprising conclusion that the O atoms of the water layer were virtually coplanar [6].

Their expectation was that O atoms would lie in *two* planes separated by about 1 Å, a "bilayer" arrangement similar to a single, (0001) layer of ice Ih. The water molecules corresponding to the lower-lying O atoms would contribute two donor H-bonds to the bilayer's hexagonal network. The other molecules would contribute one, leaving their remaining H-atoms "dangling."

To explain the observed coplanar structure, an idea was needed, not just DFT calculations. It was that in the bilayer, there is no driving force to move an upper O atom toward the surface, because an upper O atom's lone pair orbital is "used up" in forming the dangling O–D bond. Were that bond broken, the upper O atom would move down [7].

DFT calculations confirmed this notion. A half-dissociated water adlayer, with dangling O–H bonds replaced by

Ru–H bonds, not only optimized to form a nearly coplanar O structure, but also had a binding energy 0.2 eV/water molecule better than that of the undissociated bilayer [7].

Subsequent calculations of vibration energies revealed that because Ru–H bonds are softer than O–H bonds, dissociation red-shifts the spectrum, on average. As a result, zero-point energy favors the half-dissociated state by another 0.08 eV per water molecule. Thus, DFT rationalized Held and Menzel's co-planar O atom structure, and also explained why the adlayer is favored thermodynamically relative to 3-D ice, i.e., why water wets Ru(0001) at all [8].

Resolution of a then 8-year-old problem was exciting. But follow-up studies on other precious metals suggest "seductive" as the *mot juste*. Water-on-Ru is a special case, characterized by exceptionally large energy differences. On Pt(111), a surface not active enough to dissociate water molecules or even to support a beam-damaged, dissociated structure, DFT has not yielded an explanation of why first-layer wetting is preferred to formation of 3-D ice [9, 10]. On Pd(111), as explored in the next section, the ordering of DFT energies versus water adlayer arrangement seems to have little to do with actual observation. Thus, the DFT account of the half-dissociated water/Ru(0001) structure [7, 8] was somewhat unfortunate. It made what now seems the untimely question of precious metal wetting structures, appear less so.

3 Low Coverage Water on Pd(111)

Water does not form an extended wetting layer on Pd(111) [11]. Instead, according to STM imaging, "rosette" (see Fig. 1a) and "lace" islands form when H₂O is deposited at low temperature and coverage, whose sizes can be rationalized by a water molecule preference for O–H bonds to be aligned roughly parallel to the metal surface [12].

DFT calculations based on the PBE approximate functional [13] do show a small preference for water rosettes, with a lattice energy of 0.51 eV/H₂O, compared to 0.50 eV/H₂O for an extended, H-down bilayer (see Fig. 1b), and they do agree with the observation that no 2-dimensional adlayer is better bound than 3-dimensional ice Ih, whose PBE lattice energy is 0.64 eV/H₂O. But, once one investigates other single-adlayer structures, confidence in the PBE energies is harder to sustain.

Consider, e.g., a full monolayer, chain-structured adlayer (see Fig. 2), like that proposed by Hodgson and co-workers [14, 15] to account for low-temperature wetting of Ru(0001) by intact water molecules. Its PBE lattice energy is 0.54 eV/H₂O. This result is worrisome: if water molecules are mobile enough, at low temperature and coverage, to find each other and form rosettes (cf. Fig. 1a),

² Though, in fairness, its structure was first solved (in a similar time frame) by imaginative application of the transmission electron microscope (See Ref. [3]), not the STM.

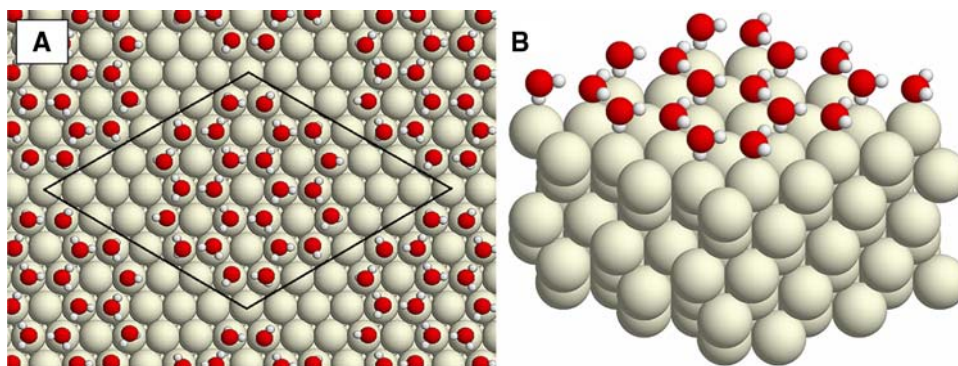


Fig. 1 (Color online) with H, O and Pd atoms represented by small, medium and large spheres, **a** Top view of an H-down, rosette island in the $4\sqrt{3} \times 4\sqrt{3} - R30^\circ$ Pd(111) supercell indicated by the black parallelogram, and **b** Oblique view of nine surface unit cells of an

extended, H-down, $\sqrt{3} \times \sqrt{3} - R30^\circ$ bilayer adsorbed on a 5-layer, Pd(111) slab. The terminology “H-down” means the dangling H atoms of the adlayer lie below O atoms

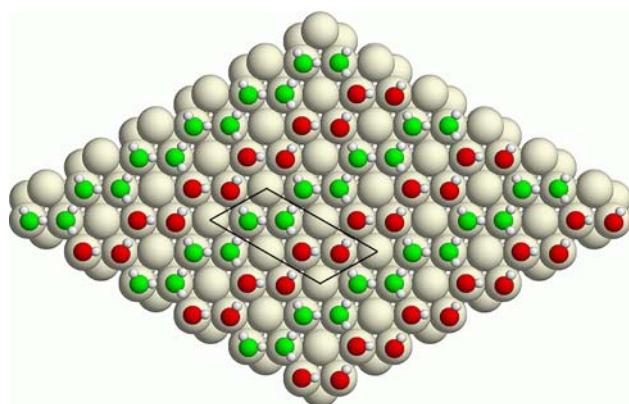


Fig. 2 (Color online) After Refs. [14] and [15], the first layer of water molecules in a periodic “chain structure,” on Ru(0001). The O atoms of flat-lying water molecules are light grey (green online). Those of H-down water molecules are dark grey (red online). H atoms are represented by white spheres and Ru atoms by light yellow. The black parallelogram delimits the $\sqrt{3} \times 2\sqrt{3} - R30^\circ$ supercell

why do they stop there, instead of gaining 30 meV each by forming large, chain-structure islands, as in Fig. 2?

Strain in water islands on Pd(111) is also a concern. In the PBE world, the ice Ih lattice constant, $a = 4.424 \text{ \AA}$, while the nearest Pd–Pd separation on Pd(111) is 2.794 \AA . The result is that a commensurate $R30^\circ$ bilayer arrangement of water molecules on the metal surface has O–O bond lengths of 2.83 \AA (flat molecules donating to H-down) and 2.78 \AA (H-down molecules donating to flat) as compared to 2.71 \AA for all the O–O bonds in PBE ice.

This means a commensurate $R30^\circ$ bilayer should experience considerable tensile stress, and might find it energetically advantageous to forego O-atom bonding in the preferred, atop sites [16] in favor of shorter H-bond lengths. The observation that water does not form a complete 2-D layer on Pd(111), supports this notion. Formation of a full 2-D layer occurs when metal–water interactions dominate water–water bonding. When water–water bonds

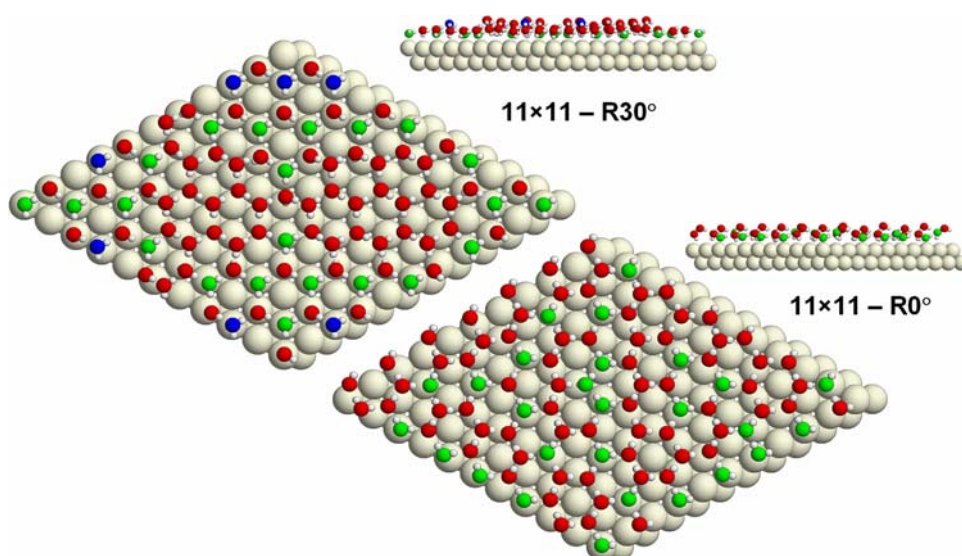
are dominant, dewetting to form 3-D structures is expected, thermodynamically. Before this happens in a water adlayer of sufficient area, one can expect tensile stress reduction to be favored, at the cost of water–metal bond strength.

To test this idea, given that H-bonded water structures have been observed on Pd(111) in both $R30^\circ$ and $R0^\circ$ orientations (S. B. Maier, I. Stass and M. Salmerón, unpublished), I sought a single supercell that would accommodate fully H-bonded, periodic water adlayers in either, with average O–H···O bond lengths comparable to those of bulk ice. Given the PBE ice Ih lattice constant $a = 4.424 \text{ \AA}$, an 11×11 Pd(111) supercell is ideal. For the $R0^\circ$ wetting layer, $7a_{\text{ice Ih}} = 30.968 \text{ \AA}$ matches the 30.734 \AA side of the Pd supercell to better than 1%. For the $R30^\circ$ wetting layer, the side of the 11×11 Pd(111) supercell is spanned by $4\sqrt{3} a_{\text{ice Ih}} = 30.65 \text{ \AA}$, an even better match. In the former case, the cell holds 98 H_2O molecules. In the latter it holds 96.³

I computed supercell wetting energies by adding H_2O molecules on top of a 2-layer Pd(111) slab, whose lower-layer atoms were fixed in a (111) plane at theoretical bulk Pd separations. The results were lattice energies of 0.53 eV and 0.54 eV per water molecule, for ordered arrangements of the H-bonds (see Fig. 3). Very similar results were obtained for sample, disordered H-bonding structures. Together they imply that the gain reaped by allowing H-bonds to adopt their preferred lengths is roughly equal to the loss because fewer O atoms than a third lie directly atop Pd atoms, in the 11×11 supercell. The relative unimportance of atop-site binding to the monolayers is

³ Note that the 11×11 Pd(111) supercell would be less ideal if the PBE functional were more representative of “real-life” lattice constants. As PBE ice is contracted by 1.7 linear percent and Pd expanded by 1.6%, for example, the mismatch for the $R0^\circ$ wetting layer would be $7a_{\text{ice Ih}} = 31.479 \text{ \AA}$ compared to a supercell side of 30.25 \AA , i.e., about 4% rather than less than 1%.

Fig. 3 (Color online) Proton-ordered water adlayers in a Pd(111) – 11×11 supercell. Upper and lower panels show $R30^\circ$ and $R0^\circ$ structures comprising 96 and 98 water molecules. Of the flat-lying water molecules whose O atoms are in near atop sites, those whose O atoms lie within 2.51 Å of the underlying Pd are colored green (27 in the $R0^\circ$ case and 31 for the $R30^\circ$), and those which lie higher are colored blue. The side view insets show the adlayers' corrugation directly



confirmed by the near equivalence of the binding energies found for the $R30^\circ$ and $R0^\circ$ orientations.

Overall, this study shows that within the PBE Generalized Gradient Approximation to DFT [13], the total energy does not predict water adlayer geometries on Pd(111). It does not distinguish commensurate from incommensurate structures, nor explain why small islands do not coalesce.

Other difficulties arise when one tries to account for the water adlayer structures found on Pt(111) [17]. DFT has provided no explanation for wetting of this surface by a single water layer, as against formation of 3-dimensional ice clusters [9, 10], and no understanding of why, at saturation, a $\sqrt{39} \times \sqrt{39} - R16.1^\circ$ wetting layer has been observed in diffraction experiments [18–20].

Thus one can use DFT-optimized surface structures to help interpret STM images of water on precious metals [12].⁴ But, we must await a more accurate functional before wetting-layer molecular arrangements will be predictable, based on DFT total energies. I have worked on the water on Pt(111) structure now for several years (see, e.g., Refs. [9, 17]), and still cannot say if my failure to find a wetting arrangement of H_2O molecules should be attributed to use of an insufficiently accurate density functional, or to failure to find the structural motif nature adopts. Such a long-term effort, with no firm conclusions, seems the very model of a quixotic endeavor!

4 Ice Nucleation on β -AgI

Nucleation of ice crystals from water vapor is a prerequisite for raindrop formation. The lower vapor pressure

⁴ For another example, water on Cu(110), see [21], and an accompanying perspective, [22].

of ice means that ice nuclei grow at the expense of nearby water droplets, and eventually become large enough to overcome friction and fall to earth.

In the late 1940s, based on his survey of crystal lattice data, Bernard Vonnegut suggested using AgI “smoke” to seed clouds with ice nuclei [23]. The idea, largely discounted by now [24], was that the good lattice match between β -AgI and ice Ih meant ice would readily nucleate on the “smoke” particles. And, in the lab, it does.

Still, it remains unproven that cloud seeding works, or does not, or that lattice match is the key property of a cloud seed, and not surface “chemistry” or the presence of some kind of crystal defect. Of interest, to promote our understanding, is whether we can address the role of good lattice match in ice nucleation by conducting DFT optimizations.

Once again underlining the need for a significantly improved approximate functional, however, a recent survey of ice Ih and β -AgI lattice constants revealed that the match is considerably worse than what is experimentally observed [25]. Among eight local (LDA) and semi-local (GGA) approximate functionals, the range of the mismatch runs from 4.2 to 7.9%, compared to the experimental 2.2%, observed near the absolute zero of temperature.

The best match is for the RPBE, GGA functional [26]. That functional, however, underestimates the lattice energy of bulk ice Ih by almost 25%, casting doubt on its ability to capture wetting energetics faithfully. The recent AM05 and PBEsol functionals [27, 28], which were developed to automate the choice between using a local functional or a GGA, both optimize ice with a mismatch to β -AgI of more than 6 linear percent, and with a lattice energy $\geq 8\%$ too large compared to experiment.

These results imply that using DFT to understand the role of lattice match in the nucleation of ice on AgI is not timely. A functional must be developed that accounts better

for H-bonding. It is worth noting, in this regard, that the weakness of van der Waals forces in the various incarnations of the Generalized Gradient Approximation is not the underlying problem. The AM05 functional, e.g., as judged by the discovery that it predicts no minimum energy graphene-layer separation along the *c*-axis of graphite, embodies no van der Waals attractive forces at all [29]. Still, that functional predicts an ice-Ih crystal too dense by 12.5% and energetically too tightly bound by 8%. Adding a van der Waals attractive correction would only exacerbate these problems.

5 Ir Clusters on Graphene/Ir(111)

A last example of the inability of commonly used density functionals to capture experimental observations concerns the morphology of Ir clusters grown by evaporating Ir atoms onto a graphene on Ir(111) “template.” In the original experiments, N’Diaye, et al. prepared single layer, graphene flakes as large as 0.3 mm across by pyrolysis of ethylene on an Ir(111) surface [30]. Subsequent deposition of Ir adatoms on top of the graphene, monitored with STM, produced regular hexagonal arrays of Ir clusters.

At low adatom coverages of roughly 0.05 ML, the clusters were found to be 2-dimensional, and to comprise about 4 Ir adatoms. Up to 6-Ir islands were always flat, but once the islands comprised about 25 Ir adatoms, at higher coverages, equal numbers of flat and three-dimensional islands were observed.

To account for the regularity and stability of the Ir cluster arrays seen by N’Diaye, et al., I began by performing DFT optimizations, using the PW91 version of the GGA [31–33]. The disappointing result was the prediction that even four-Ir islands should prefer to grow three-dimensionally, i.e., as trigonal pyramids, rather than flat, i.e., as rhombi [34]. Apparently, in the PW91 universe, the Ir–Ir attraction is sufficiently strong, compared to that between Ir and C atoms, that even a 4-Ir island will prefer not to “wet” the graphene below it.

If one uses the Ceperley–Alder, local density approximation,⁵ (the CA-LDA) the opposite is true. In the CA-LDA world, small Ir adatom clusters on graphene/Ir(111) should remain flat, thermodynamically. As the clusters gain more atoms, they spread and eventually encroach into regions of the graphene adlayer where (because of lattice mismatch to the underlying Ir metal surface) buckling of the graphene layer to allow formation of C bonds to Ir atoms directly below them cannot occur. At that point, Ir–C bonding weakens, and formation of a 2-layer Ir cluster becomes favored by a non-linear increase in the number of

Ir–Ir bonds. Accordingly, there is a crossover from 2-D to 3-D Ir cluster formation. Experimentally, it occurs at roughly 25 Ir adatoms, as noted. Using the CA-LDA functional, the transition occurs at 26 Ir adatoms—in good agreement with observation [37].

The satisfying conclusion is that the CA-LDA appears to capture the energetics needed to explore the morphology of N’Diaye, et al.’s cluster arrays. Less satisfying is that GGA calculations using the PW91 functional fail to account for a feature as basic as the shape of a small Ir cluster. Thus, although one might use the CA-LDA to explore further, e.g., to study cluster growth kinetics, one cannot claim that DFT is predictive. Choose the wrong functional, and the results of cluster optimization may be not just quantitatively, but qualitatively incorrect. This is a situation that, once again, begs for the development of a more universally applicable functional.

6 Lessons Learned

Density Functional Theory has been extremely valuable over the past 30 years in the quest to understand the structure and behavior of condensed matter systems. Still, poorly controlled systematic error in the approximate functionals available today requires that one consider which problems are likely to benefit from the application of DFT studies and which remain untimely. The success Nørskov and collaborators have had in applying DFT to the search for improved, economical catalyst materials, rightly celebrated in this symposium, speaks directly to the issue of DFT error versus timeliness. They explain: [38]

“The volcano-shaped relationships between total catalytic rates and adsorption energies may explain some of the good agreement between experiments and theory.... Close to the top...the rate depends only weakly on the absolute strength of the adsorption energies.... This means that for the best catalysts...errors of a few tenths of an eV may still give reasonable values for the rate. As this is the typical error of DFT calculations [26], they can give quite accurate rates at least close to the top of the volcano.”

Nørskov, et al. also point out that from a practical perspective, if one can use DFT results to reduce the number of candidate catalysts for a given process from thousands to a couple of dozen, that is a serious contribution. It is not necessary, although desirable, to be able to reduce the candidate set to one or two. This perspective also reduces the demands on the error level of DFT.

For problems where we do not yet possess such clear insight, or are interested in greater molecular-level detail, framing timely problems and pushing untimely ones to the

⁵ See [35], as parameterized by Perdew and Zunger [36].

back burner is essential to research productivity. The examples discussed in this article teach that:

- (1) Where energy differences are substantial,⁶ DFT energetics is likely to provide correct structural predictions, e.g., for half-dissociated water on Ru(0001). But,
- (2) In the “real world” of ambient temperature and pressure systems, such cases may be exceptional, and thus not so “important.”
- (3) When energy differences are small, direct comparison of DFT results to data (STM, Infra-red absorption spectroscopy, etc.) may allow interpretation even when the DFT total energies are unhelpful, e.g., for water on Pd(111) [12, 21, 22]. Still, being able to use the energies remains a priority. For an important example, without predictive energies, molecular dynamics simulation loses its meaning.
- (4) In some cases (“back-burner” problems), we may just have to wait for a better functional, e.g., for ice epitaxy on β -AgI [25].
- (5) The vision of systematic improvement in functionals (“Jacob’s Ladder” [40]) is appealing. But “improved” functionals may be less faithful to experiment than older ones. Two examples provided herein, concern Ir on graphene/Ir(111) [30, 34], and ice epitaxy on β -AgI [25].

And so, at the risk of truism, there are two ways to advance the contributions of DFT to condensed matter physics and chemistry. One is to develop enough insight to distinguish problems where the error level of today’s functionals does not stand in the way of drawing valuable inferences. The other is to devote more effort to reducing DFT systematic error.

Acknowledgments This work was supported by the U. S. Department of Energy, Office of Basic Energy Sciences, Division of Materials Science and Engineering. Sandia is operated by the Lockheed Martin Co. for the U.S. DOE’s National Nuclear Security Administration under contract DE-AC04-94AL85000.

References

1. Binnig G, Rohrer H, Gerber Ch, Weibel E (1982) *Phys Rev Lett* 49:57
2. Marcus PM (1994) *Surf Sci* 299/300:447
3. Takayanagi K, Tanishiro Y, Takahashi M, Takahashi S (1985) *J Vac Sci Tech* 3:1502

4. Hohenberg P, Kohn W (1964) *Phys Rev* 136:B864
5. Kohn W, Sham LJ (1965) *Phys Rev* 140:A1133
6. Held G, Menzel D (1994) *Surf Sci* 316:92
7. Feibelman PJ (2002) *Science* 295:99
8. Feibelman PJ (2003) *Phys Rev* B67:035420
9. Feibelman PJ (2003) *Phys Rev Lett* 91:059601
10. Meng S, Xu LF, Wang EG, Gao S (2002) *Phys Rev Lett* 89:176104
11. Henderson MA (2002) *Surf Sci Rep* 46:1, Table 4
12. Cerda J, Michaelides A, Bocquet ML, Feibelman PJ, Mitsui T, Rose M, Fomin E, Salmeron EM (2004) *Phys Rev Lett* 93:116101
13. Perdew JP, Burke K, Ernzerhof M (1996) *Phys Rev Lett* 78:3865
14. Haq S, Clay C, Darling GR, Zimbitas G, Hodgson A (2006) *Phys Rev B* 73:115414
15. Gallagher M, Omer A, Darling GR, Hodgson A (2009) *Farad Discuss* 141:231
16. Michaelides A, Ranea VA, de Andres PL, King DA (2003) *Phys Rev Lett* 90:216102
17. Feibelman PJ (2009) *Farad Discuss* 141:467
18. Glebov A, Graham AP, Menzel A, Toennies JP (1997) *J Chem Phys* 106:9382
19. Haq S, Harnett J, Hodgson A (2002) *Surf Sci* 505:171
20. Zimbitas G, Haq S, Hodgson A (2005) *J Chem Phys* 123:174701
21. Carrasco J, Michaelides A, Forster M, Haq S, Raval R, Hodgson A (2009) *Nat Mat* 8:427
22. Feibelman PJ (2009) *Nat Mat* 8:372
23. Vonnegut B (1947) *J Appl Phys* 18:593
24. Pruppacher HR, Klett JD (1997) *Microphysics of clouds and precipitation*. Kluwer Academic Publishers, Norwell, MA, 2nd Enlarged and Revised Edition, Table 9.7, p 332
25. Feibelman PJ (2008) *Phys Chem Chem Phys* 10:4688
26. Hammer B, Hansen LB, Nørskov JK (1999) *Phys Rev B* 59:7413
27. Armiento R, Mattsson AE (2005) *Phys Rev B* 72:085108
28. Perdew JP, Ruzsinszky A, Csonka GI, Vydrov O, Scuseria GE, Constantin LA, Zhou X, Burke K (2008) *Phys Rev Lett* 100:136406
29. Haas P, Tran F, Blaha P (2009) *Phys Rev B* 79:085104
30. N’Diaye AT, Bleikamp S, Feibelman PJ, Michely T (2006) *Phys Rev Lett* 97:215501
31. Perdew JP (1991) In: Ziesche P, Eschrig H (eds) *Electronic structure of solids ’91*. Akademie Verlag, Berlin
32. Perdew JP, Chevary JA, Vosko SH, Jackson KA, Pederson MR, Singh DJ, Fiolhais C (1992) *Phys Rev B* 46:6671
33. Perdew JP, Chevary JA, Vosko SH, Jackson KA, Pederson MR, Singh DJ, Fiolhais C (1993) *Phys Rev B* 48:4978
34. Feibelman PJ (2008) *Phys Rev B* 77:165419
35. Ceperley DM, Alder BJ (1980) *Phys Rev Lett* 45:566
36. Perdew JP, Zunger A (1981) *Phys Rev B* 23:5048
37. Feibelman PJ (2009) *Phys Rev B* 80:085312
38. Nørskov JK, Bligaard T, Rossmeisl J, Christensen CH (2009) *Nat Chem* 1:37
39. Feibelman PJ, Hammer B, Nørskov JK, Wagner F, Scheffler M, Stumpf R, Watwe R, Dumesic J (2001) *J Phys Chem B* 105:4018
40. Perdew JP, Schmidt K (2001) *AIP Conf. Proc.*, vol 577, p 1

⁶ Though, see, e.g., [39], how substantial is not easy to specify.